23rd ABCM International Congress of Mechanical Engineering
December 6-11, 2015, Rio de Janeiro, RJ, Brazil

INFLUENCE OF THE LUBRICATION MODEL ON THE DYNAMIC BEHAVIOR OF SLIDER-CRANK MECHANISM WITH CLEARANCE

Lucas Tavares Selegatto[1]
ltselegatto@fem.unicamp.br
Vitor Luiz Reis[2]
vreis88@gmail.com
Gregory Bregion Daniel[1]
gbdaniel@fem.unicamp.br
[1]Laboratory of Rotating Machinery – Faculty of Mechanical Engineering – Postal Box 6122
University of Campinas (UNICAMP)
13083-970, Campinas, SP, Brazil
[2]Aeronautics Institute of Technology (ITA)
12228-900, São José dos Campos, SP, Brazil

Abstract. *Slider-crank mechanisms are employed in many machines, such as engines, compressors and pumps. Thus, the dynamic analysis of these mechanisms is very important, since the occurrence of problems directly affect their performance and lifetime. For this reason, this work aims to evaluate the influence of different lubrication models in the dynamic behavior of slider-crank mechanism with clearance on the piston-pin revolute joint. Thereby, the dynamic model of the mechanism is obtained by Lagrange's method, considering the contact, friction and lubrication effects on the piston-pin revolute joint. In this approach, the Hertz contact model and the Coulomb friction model were considered. For hydrodynamic lubrication, analytical models were adopted for short bearing (Frene's model) and for long bearing (Pinkus and Sternlicht's model), besides the numerical model where the hydrodynamic force is obtained from solution of Reynolds equation. The results presented in this work show the influence of the lubrication models in the dynamic behavior of the mechanism and the lubrication conditions in the pin-piston revolution joint, emphasizing the differences between the hydrodynamic forces obtained from analytical and numerical models.*

Keywords: *Hydrodynamic Lubrication, Hydrodynamic Forces, Slider-Crank Mechanism*

1. INTRODUCTION

The analysis of the dynamic behaviour of mechanisms is an important task of machinery design, especially when its operation regime occurs at high speeds and/or subjected to rigorous tolerances of movement. An example of such machine is the slider-crank mechanism commonly used in internal combustion engines, compressors and pumps.

The joints that allow the relative motion between its links also introduce clearances that inevitably lead to wear and vibration, decreasing the overall mechanism performance. The treatment of the clearance in multibody dynamics was also extended to include the effect of lubrication (Flores *et al.* 2009, Tian *et al.* 2011 and Daniel and Cavalca 2011). In tribology, the hydrodynamic forces generated on the fluid film inside the bearing are dependent of the squeeze and wedge effects (Tian *et al.* 2013). For low relative velocities between the journal and the bearing, the squeeze film effect becomes dominant and the approximate solution obtained for long bearing in this situation (Flores *et al.* 2004) predicted a smoothed dynamic response of the mechanism in comparison to a dry clearance.

However, for high relative velocities, the simple squeeze approach is not valid and, consequently, the Reynolds equation should be applied. Flores *et al.* (2009) and Machado *et al.* (2012) presented results for dynamic simulations using hydrodynamic lubrication models based on the closed solutions of the Reynolds equation, for long and short bearings, both for Gumbel and Sommerfeld boundary conditions.

Tian *et al.* (2011) simulated the behaviour of planar flexible multibody systems using the Absolute Nodal Coordinate Formulation (ANCF) with clearance and lubricated revolute joints. The results obtained showed the importance of modelling flexibility of the links especially for “soft” materials.

Daniel and Cavalca (2011) and Reis *et al.* (2014) also analysed the dynamic of a slider–crank mechanism with lubrication in the connecting rod–slider joint clearance. Using the hydrodynamic lubrication model for long bearings with alternate motion (Bannwart *et al.* 2010), their results indicate that the wedge effect itself is not capable to sustain the journal in hydrodynamic lubrication during the simulations.

In this work the influence of hydrodynamic force model was investigated on the response of the slider-crank mechanism. Analyses comparing the analytical solutions for short bearing (Frene’s model) and for long bearing (Pinkus and Sternlicht's model) with those obtained from the numerical model where the hydrodynamic forces are obtained from the solution of Reynolds equation. The results shows the influence of the lubrication models in the dynamic behaviour of the mechanism and the lubrication conditions in the pin-piston revolution joint, emphasizing the differences between the hydrodynamic forces obtained from analytical and numerical models.

2. METHODOLOGY

In this section, the methodology applied in this work is briefly exposed. Firstly, the equations that describe the dynamic behavior of the system are presented. In following, the lubrication models adopted in the analytical solutions, for long and short journal bearings, and numerical solution, from the classical Reynolds equation, are shown.

2.1 Dynamic equations of the mechanism

A classical slider-crank mechanism is known for having a single degree of freedom and a planar motion. The consideration of a clearance in the piston-pin joint (journal bearing) does not change the planar motion characteristic, however, it adds two degrees of freedom to the system. In this case, its independent coordinates can be: the crank angular displacement (q), the connecting rod angular displacement (A), and the slider displacement (X_{PT}). Figure 1 shows an scheme of the mechanism and highlights the hydrodynamic bearing considered in the piston-pin joint.

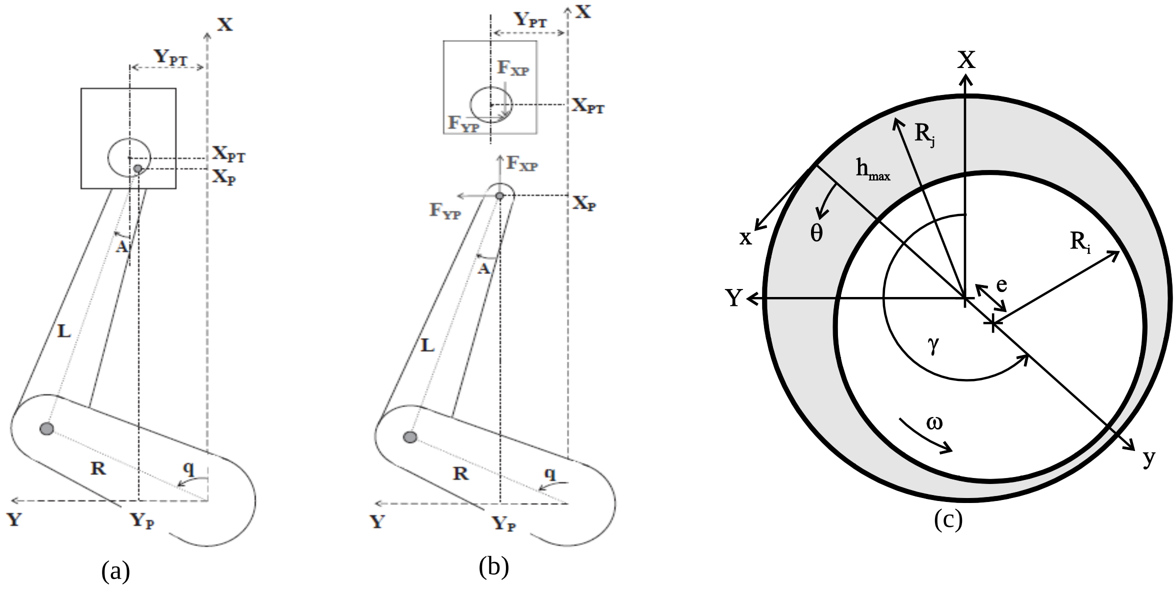

Figure 1: Scheme of the slider-crank mechanism. (a) Planar view. (b) Planar view with the forces over each component. (c) Hydrodynamic bearing modeling the piston-pin joint. (Daniel and Cavalca, 2011; Reis *et al*., 2014).

Defining I_{MO} and I_B as the crank and connecting rod rotational inertias and applying Lagrange's formulation, the equation of motion for the complete mechanism is given by Eq. (1) (Daniel and Cavalca, 2011):

$$\begin{gathered}
\begin{bmatrix} M_B R^2 + I_{M0} & -M_B R\left(U_{PB}\cos(A+q) + V_{PB}\sin(A+q)\right) \\ \text{sym} & M_B\left(U_{PB}^2 + V_{PB}^2\right) + I_B \end{bmatrix} \begin{Bmatrix} \ddot{q} \\ \ddot{A} \end{Bmatrix} + \\
+ M_B R\left(V_{PB}\cos(A+q) - U_{PB}\sin(A+q)\right) \begin{Bmatrix} \dot{A}^2 \\ \dot{q}^2 \end{Bmatrix} + \\
+ g \begin{Bmatrix} M_M\left(-U_{PM}\sin(q) - V_{PM}\cos(q)\right) - M_B R\sin(q) \\ M_B\left(-U_{PB}\sin(A) + V_{PB}\cos(A)\right) \end{Bmatrix} = \begin{Bmatrix} F_{yp}R\cos(q) - F_{xp}R\sin(q) - \tau_d \\ -F_{yp}L\cos(A) - F_{xp}L\sin(A) \end{Bmatrix} \\
M_{PT}\ddot{X}_{PT} = -\left(F_{ext} + gM_{PT} + F_{xp}\right)
\end{gathered} \tag{1}$$

In the set of equations numbered as (1), g is the gravitational acceleration; M_M is the crank mass; M_B is the connecting rod mass; M_{PT} is the slider mass; U_{PMI} and V_{PMI} are the coordinates of the crank center of mass in the local reference system (U_M, V_M); U_{PB} and V_{PB} are the coordinates of the connecting rod center of mass in the local reference system (U_B, V_B); X_{PM} and Y_{PM} are the displacements of the crank's center of mass, X_{PB} and Y_{PB} are the displacements of the connecting rod's center of mass and X_{PT} is the displacement of the piston, in relation to the inertial reference system (X,Y). The meanings of the remaining parameters can be inferred from the indications in Fig. 1, previously exposed.

The system behavior is strongly dependent on the relative motion between the connecting rod and the slider, being linked by a revolute joint modeled as a journal bearing. The pin eccentricity in the bearing is composed by radial displacements in the directions x and y as presented in Eq. (2):

$$e = \sqrt{e_x^2 + e_y^2} \tag{2}$$

These displacements are evacuated by the relative position between the slider and the pin.

$$\begin{Bmatrix} e_x \\ e_y \end{Bmatrix} = \begin{Bmatrix} X_p - X_{PT} \\ Y_p - Y_{PT} \end{Bmatrix} \tag{3}$$

Moreover, the eccentricity ratio and its variation in time are defined, respectively, as:

$$\varepsilon = \frac{e}{c_r} \quad ; \quad \dot{\varepsilon} = \frac{\dot{e}}{c_r} \tag{4}$$

Finally, it is necessary to determine the attitude angle, just like its variation in time.

$$\gamma = atan2\left(\frac{e_y}{e_x}\right) \quad ; \quad \dot{\gamma} = \frac{e_x \dot{e}_y - e_y \dot{e}_x}{e^2} \tag{5}$$

2.2 Lubrication models

Depending on the length-diameter ratio, the journal bearing can be considered as infinitely long, infinitely short and finite. Long bearing approximation can be used when the flow in the axial direction is practically null, causing a null pressure gradient in such direction. On the other hand, short bearing approximation can be used when the flow in the circumferential direction is practically null and, consequently, the pressure gradient is also null in such direction. Lastly, finite bearing presents flows in both directions and, consequently, there are pressure gradients in both directions. In this case, a numerical method must be applied to obtain the pressure distribution, since it has no analytical solution.

All three cases just presented arise from the Reynolds equation (Reynolds, 1886) presented in Eq.(6). The x and z coordinates represent the circumferential and axial directions, respectively. As previously described, the first term in the left side of the equation is neglected for short bearings while the second term is neglected for long bearing.

$$\frac{\partial}{\partial x}\left(h^3 \frac{\partial P}{\partial x}\right) + \frac{\partial}{\partial z}\left(h^3 \frac{\partial P}{\partial z}\right) = 6\mu U \frac{\partial h}{\partial x} + 12\mu \frac{\partial h}{\partial t} \tag{6}$$

The oil film thickness (h) can be obtained from the eccentricity ratio and radial clearance, as presented in Eq. (7).

$$h(\theta) = c_r(1 + \varepsilon.\cos(\theta)) \tag{7}$$

For short bearings, Frêne's model using the Gümbel's boundary condition is adopted. In this case, the pressure is integrated in half film (from zero to π) and, in the others parts, the pressure is set as equal to zero. The solution for the pressure distribution is presented in Eq. (8) (Frêne, 1997).

$$p(x,z) = -\frac{3\mu}{h^3}\left[\frac{{L_j}^2}{4} - Z^2\right]\left[(\omega - 2\dot{\gamma})\frac{\partial h}{\partial x} + 2\dot{\varepsilon}\cos\theta\right] \tag{8}$$

Hence, the hydrodynamic forces in the local reference system are calculated by integration of the pressure distribution, according to Frêne (1997). The hydrodynamic forces can be calculated as shown in Eq. (9), where L_j and R_j represent the length and the radius of the bearing, respectively.

$$\begin{Bmatrix} F_y \\ F_x \end{Bmatrix} = \begin{Bmatrix} -\dfrac{\mu {L_j}^3 R_j}{2{c_r}^2(1-\varepsilon^2)^2}\left[\dfrac{\pi\dot{\varepsilon}(1+2\varepsilon^2)}{\sqrt{1-\varepsilon^2}} + 2\varepsilon^2(\omega - 2\dot{\gamma})\right] \\ \dfrac{\mu {L_j}^3 R_j \varepsilon}{2{c_r}^2(1-\varepsilon^2)^2}\left[4\dot{\varepsilon} + \dfrac{\pi}{2}\sqrt{1-\varepsilon^2}(\omega - 2\dot{\gamma})\right] \end{Bmatrix} \tag{9}$$

For long bearing, the lubrication model proposed by Pinkus and Sternlich (1961) is considered in this work. This theory considers the relative motion between the journal and the bearing and also squeeze and wedge effects. Resolving the Reynolds equation adapted to long bearing, the pressure distribution can be obtained as presented in Eq. (10):

Considering an angular velocity ω of the journal, the following relations are defined:

$$p = 6\mu\left(\frac{R_j}{c_r}\right)^2 \left\{\frac{(\omega - 2\dot{\gamma})(2 + \varepsilon cos\theta)\, \varepsilon\, sin\theta}{(2+\varepsilon^2)(1+\varepsilon\cos\theta)^2} + \frac{\dot{\varepsilon}}{\varepsilon}\left[\frac{1}{(1+\varepsilon\cos\theta)^2} - \frac{1}{(1+\varepsilon)^2}\right]\right\} \tag{10}$$

Integration of the pressure distribution leads to the hydrodynamic forces acting on the bearing. The sets of equations in the sequence express these forces for the cases in which the parameter E is positive and negative, respectively.

$$\begin{Bmatrix} F_y \\ F_x \end{Bmatrix} = \begin{Bmatrix} -\frac{1}{2}\frac{\mu w R_j^3 \omega}{c_r^2}\frac{3E}{(2+\varepsilon^2)(1-\varepsilon^2)(1-\varepsilon^2)^{0.5}}\left[4k\varepsilon^2 + (2+\varepsilon^2)\pi\frac{k+3}{k+3/2}\right] \\ -\frac{1}{2}\frac{\mu w R_j^3 \omega}{c_r^2}\frac{6\pi\varepsilon(1-G)}{(2+\varepsilon^2)(1-\varepsilon^2)^{0.5}}\left(\frac{k+3}{k+3/2}\right) \end{Bmatrix} \tag{11}$$

$$\begin{Bmatrix} F_y \\ F_x \end{Bmatrix} = \begin{Bmatrix} +\frac{1}{2}\frac{\mu w R_j^3 \omega}{c_r^2}\frac{3E}{(2+\varepsilon^2)(1-\varepsilon^2)(1-\varepsilon^2)^{0.5}}\left[4k\varepsilon^2 - (2+\varepsilon^2)\pi\frac{k}{k+3/2}\right] \\ -\frac{1}{2}\frac{\mu w R_j^3 \omega}{c_r^2}\frac{6\pi\varepsilon(1-G)}{(2+\varepsilon^2)(1-\varepsilon^2)^{0.5}}\left(\frac{k}{k+3/2}\right) \end{Bmatrix} \tag{12}$$

Where the parameters E, G and k are:

$$E = \frac{2}{\omega}\dot{\varepsilon} \quad ; \quad G = \frac{2}{\omega}\dot{\gamma} \quad ; \quad k = (1-\varepsilon^2)^{0.5}\left[\left(\frac{1-G}{E}\right)^2 + \frac{1}{\varepsilon^2}\right]^{0.5} \tag{13}$$

Lastly, the numerical solution is obtained for solving the classical Reynolds equation from the Finite Volume Method (FVM). Using the computational mesh, the pressure in the interest volume (P) is obtained from the adjacent volumes (E: eastern; W: western; N: northern; S: southern) and the source term (B) (Maliska, 2004). Thus, the pressure distribution can be obtained as shown in Eq. (14).

$$C_P P_P = C_E P_E + C_W P_W + C_N P_N + C_S P_S + B \tag{14}$$

Where the coefficients in Eq.(14) are determined as in the sequence.

$$\begin{gathered} C_E = \frac{\Delta z}{\Delta x}\left(\frac{{h_e}^3}{\mu}\right); \ C_W = \frac{\Delta z}{\Delta x}\left(\frac{{h_w}^3}{\mu}\right); \ C_N = \frac{\Delta x}{\Delta z}\left(\frac{{h_n}^3}{\mu}\right); \ C_S = \frac{\Delta x}{\Delta z}\left(\frac{{h_s}^3}{\mu}\right); \\ C_P = C_E + C_W + C_N + C_S\,; \quad B = -6U[h_e - h_w] - 12\frac{\partial h}{\partial t}\Delta x \Delta z \end{gathered} \tag{15}$$

As previously mentioned, the hydrodynamic forces can be obtained from the pressure distribution. Thus, the Eq.(16) presents how to obtain the hydrodynamic forces in the local reference system and, after that, the determination of the hydrodynamic forces in the inertial reference system. The forces decomposition from the local to inertial system is the same for all models used in the work.

$$\begin{Bmatrix} F_x \\ F_y \end{Bmatrix} = \begin{Bmatrix} \sum_{i=1}^{N_x}\sum_{j=1}^{N_Z} -P_P \sin(\theta)\,\Delta x \Delta z \\ \sum_{i=1}^{N_x}\sum_{j=1}^{N_Z} P_P \cos(\theta)\,\Delta x \Delta z \end{Bmatrix} \quad ; \quad \begin{Bmatrix} F_X \\ F_Y \end{Bmatrix} = \begin{Bmatrix} F_x \sin(\gamma) + F_y \cos(\gamma) \\ F_x \cos(\gamma) - F_y \sin(\gamma) \end{Bmatrix} \tag{16}$$

3. RESULTS

The computational simulations performed in this work aim to compare the analytical solutions with the numerical solution of the Reynolds equation, allowing to evaluate how representative the models for short and long bearings are. The slider crank mechanism considered in these simulations is the same mechanism used by Reis et al. (2014), in which the geometrical parameters is presented in Table 1.

In this work, the initial velocity of the crank was 250 rad/s, and the system started from top dead center. All results are plotted after 4 laps of the crank, in order to guarantee the steady state of the system response. The equations of motion were integrated in time, using a Predictor–Corrector integrator (Shampine and Gordon, 1975), largely applied in dynamic simulations of nonlinear systems. This integrator works with a variable time-step and with an error control.

Firstly, the comparison for short bearing is presented. Figure 2(a) shows the oil film thickness and the pin's orbit inside the bearing. According to Fig. 2(b), the pin's trajectory is not the same for both solutions, although the minimum film thickness located in the superior region is similar in both cases. During the analysis, the pin is only in lubrication condition inside the bearing, i.e. there is no contact between pin and bearing. In general way, the result obtained from the analytical solution presents greater eccentricity than the results obtained from numerical solution, except in the inferior region of the bearing. Moreover, the orbits obtained in both solutions are not completely synchronized, since the trajectories are not the same. For this reason, the analytical solution considers that the pin stays more time in the critical region (minimum oil film thickness) than the numerical solution, as shown in Fig. 2(a).

Table 1. Geometrical parameters considered in the slider-crank mechanism and in the bearing.

Slider-crank Mechanism's Parameters	Values	Bearing's Parameters	Values
Crank length	0.0508 m	Bearing's diameter	0.020 m
Connecting rod Length	0.2032 m	Radial Clearance	20.10^{-6} m
Crank inertia	0.006 Kg.m	Absolute viscosity	0.0117 Pa.s
Connecting rod inertia	0.010 Kg.m	L_j/D_j Ratio for short bearing	0.2
Crank mass	0.80 Kg	L_j/D_j Ratio for long bearing	2.0
Connecting rod mass	1.36 Kg		
Slider mass	0.91 Kg		
Position of the crank center of mass in axis U_M	0 m		
Position of the crank center of mass in axis V_M	0 m		
Position of the connecting rod center of mass in axis U_B	0.0508 m		
Position of the connecting rod center of mass in axis V_B	0 m		

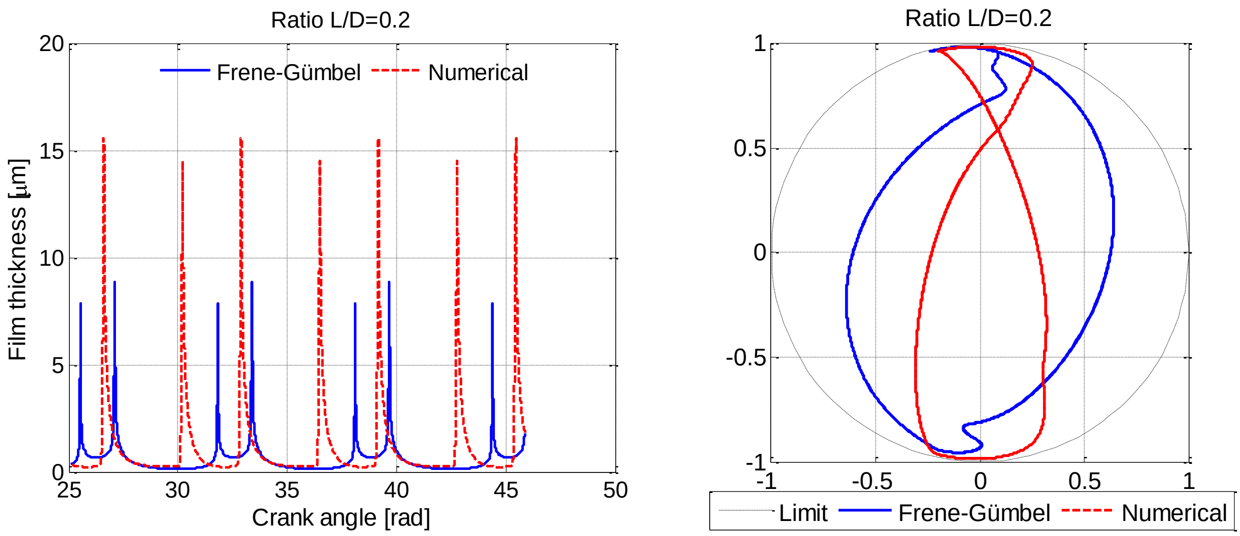

(a) (b)

Figure 2: Comparison using different solutions for short bearing (a) Oil film thickness (b) Pin's Orbit.

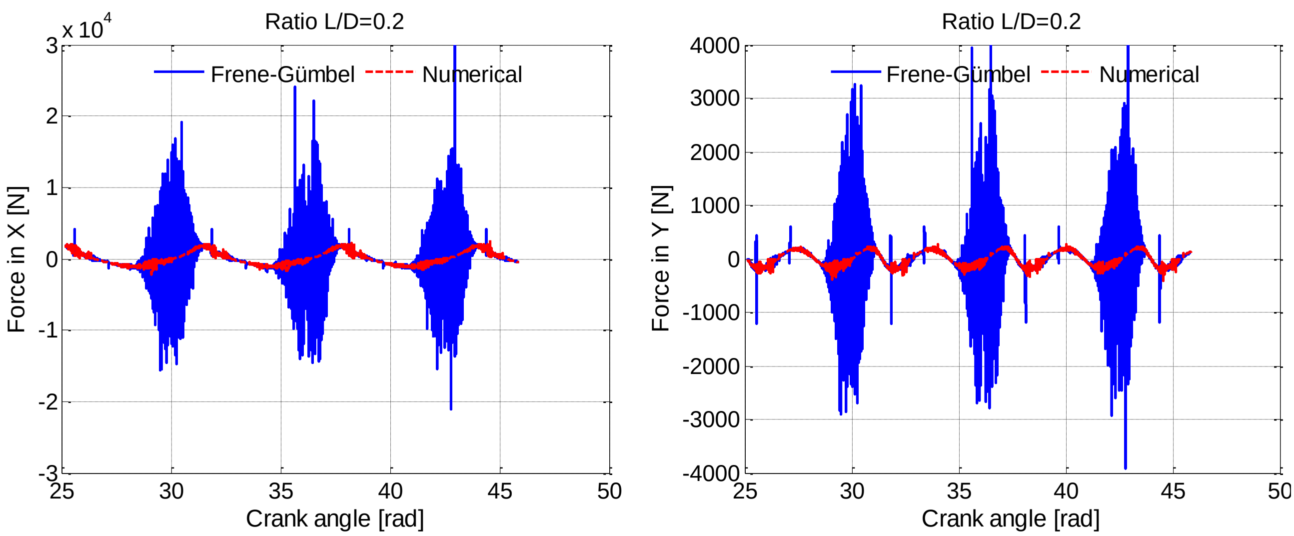

(a) (b)

Figure 3: Comparison using different solutions for short bearing (a) Force in X direction (b) Force in Y direction.

The hydrodynamic forces obtained in both solutions are shown in Fig. 3. According to Fig. 3, the tendencies of the hydrodynamic forces are similar in both directions X and Y. However, the hydrodynamic forces obtained from the analytical solution presents numerical oscillations when the pin and the bearing are critically close. This behavior can be consequence of the model sensitivity, because at the higher eccentricity levels the system of equations becomes stiff. In Fig. 4(b), the influence of these oscillations in the hydrodynamic forces can be observed in the dynamic behavior of the slider crank mechanism, mainly in the slider due to be the component where the bearing is located. On the other hand, this influence cannot be verified in the crank angular velocity obtained from the analytical and numerical solutions, since the numerical oscillations are not present in the response, as shown in Fig. 4(a).

As mentioned, the computational simulations were performed considering the slider initially located at the top dead center and the crank's initial angular velocity of 250 rad/s, as initial conditions. However, the crank angular velocity varies due to the inertial of the system during the operation, as can be seen in Fig. 4(a).

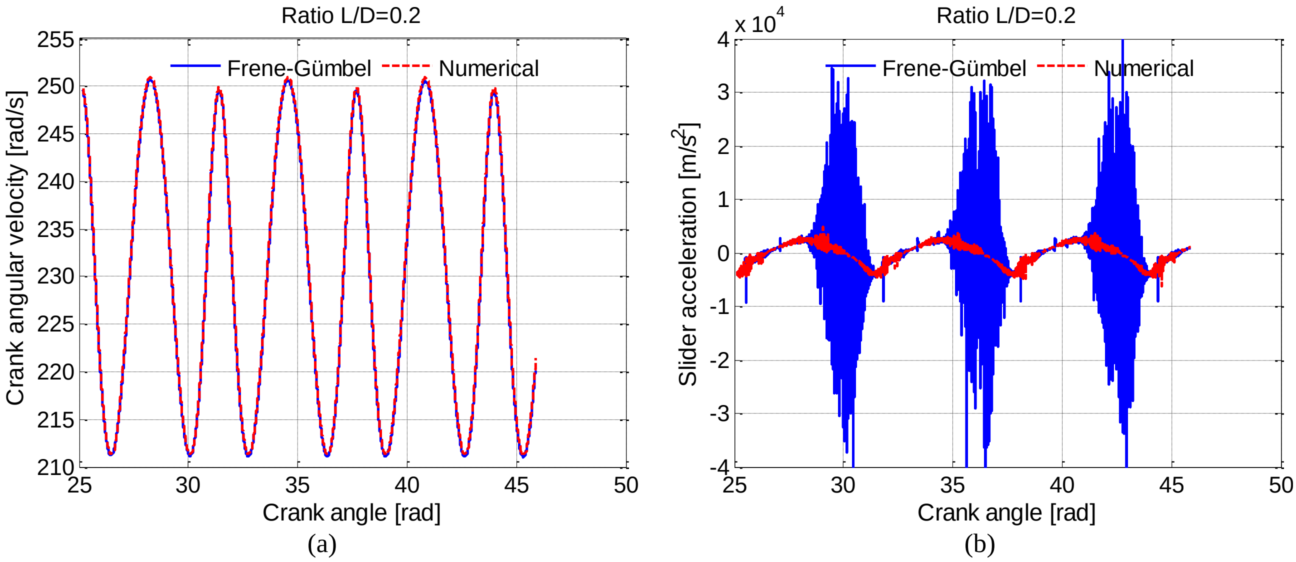

Figure 4: Comparison using different solutions for short bearing (a) Crank angular velocity (b) Slider acceleration.

For long bearings, the results obtained from the analytical and numerical solutions have better agreement. However, Fig. 5(b) shows that the pins trajectories (orbits) inside the bearing have some differences, although the dynamic behavior is similar for both solutions. The eccentricity obtained from the analytical solution is higher, causing a lower oil film thickness in the bearing, as can be seen in Fig. 5(a). Compared with short bearing, the orbits obtained in the long bearing are lower because the long bearing presents higher load capacity. In this case, the hydrodynamic forces obtained in the short bearing can be obtained from lower values of eccentricity in the long bearing; due to the bearing length is higher.

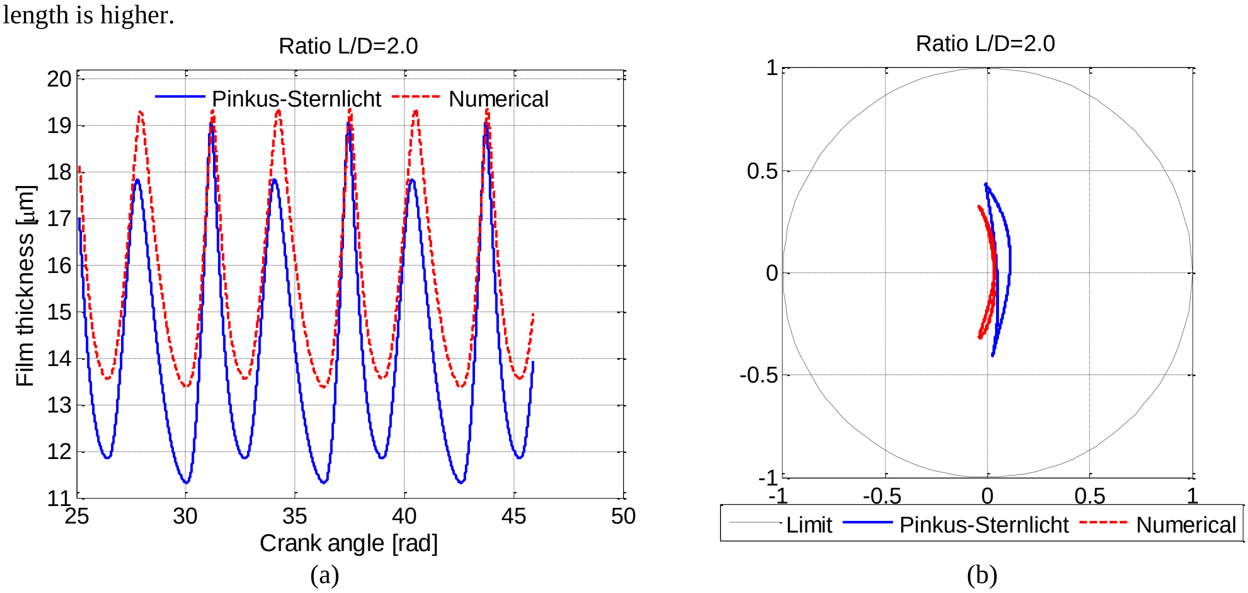

Figure 5: Comparison using different solutions for long bearing (a) Oil film thickness (b) Pin’s Orbit.

Figure 6 shows the hydrodynamic forces obtained from the analytical and numerical solutions for long bearing. In this case, a good agreement can be verified in both directions (X and Y), showing that the Pinkus-Sternlich model can represent efficiently the lubrication conditions in the joint. As also occurred in short bearing, the hydrodynamic forces in X direction is higher due to linear motion of the slide in this direction. As shown in Fig. 6(b), the hydrodynamic forces have small numerical oscillation for both solutions in the Y direction, although lower than observed in the simulations for short bearing. Also in this case, the influence of these oscillations of hydrodynamic forces can be observed in the dynamic behavior of the slider while no influence can be verified in the crank angular velocity. As previously described, the hydrodynamic forces have more influence in the slider because the bearing is located at the connecting rod-slider joint.

Lastly, it is important to highlight that the variations of the crank angular velocity are the same for computational simulations using short and long bearings, as can be verified in Figs. 4 and 7. In fact, this behavior is already expected, since the slider crank mechanism does not change and these variations occur due to the inertial of system, as previously mentioned.

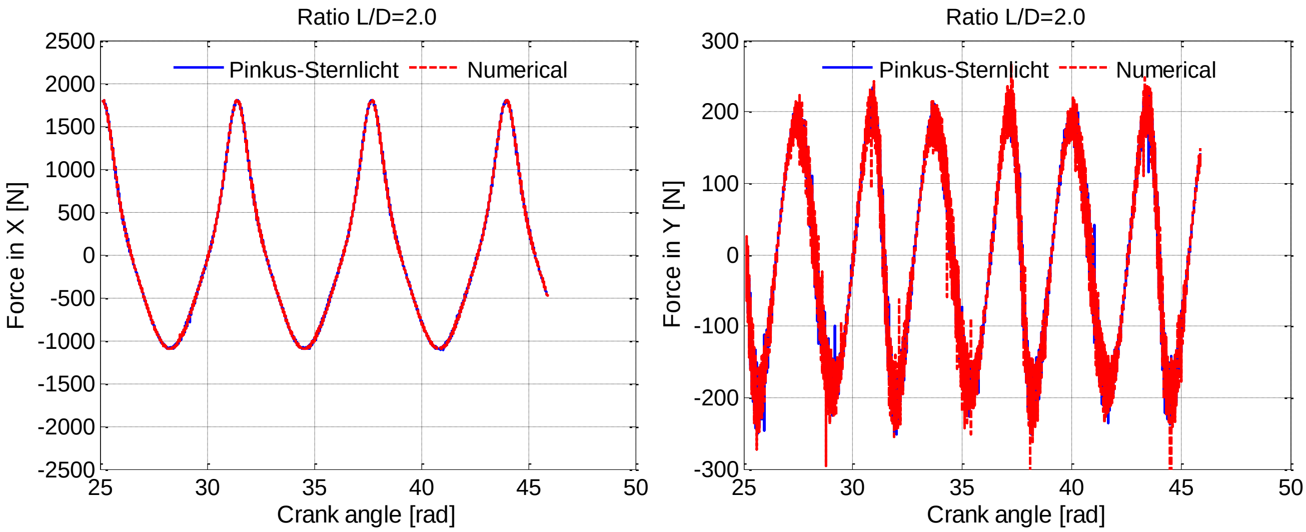

(a) (b)

Figure 6: Comparison using different solutions for long bearing (a) Force in X direction (b) Force in Y direction.

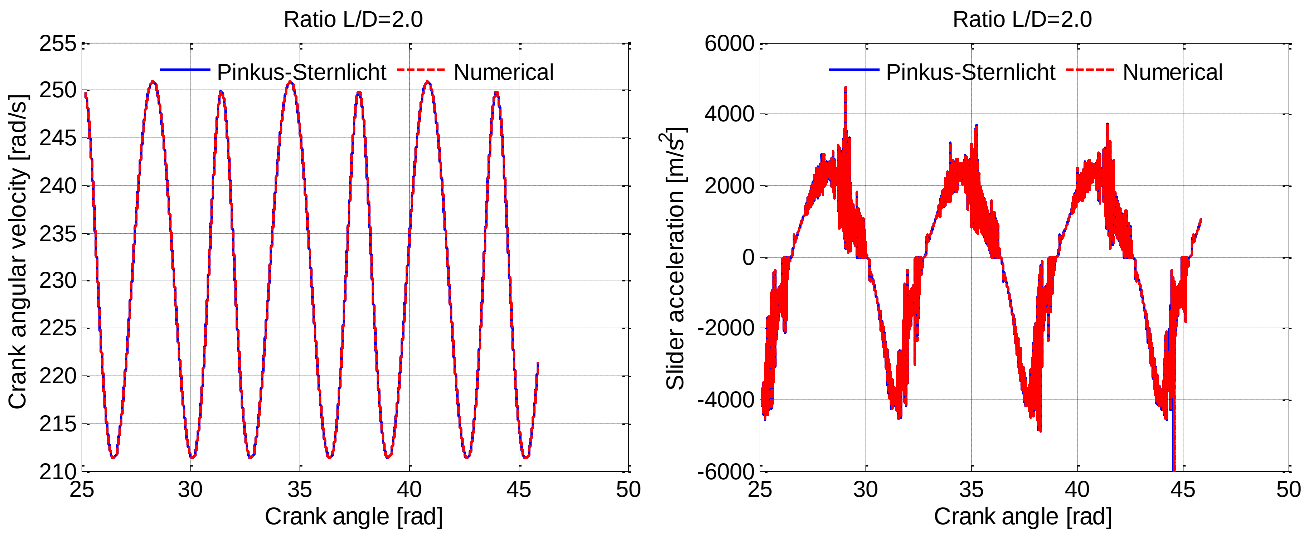

(a) (b)

Figure 7: Comparison using different solutions for long bearing (a) Crank angular velocity (b) Slider acceleration.

4. CONCLUSION

In this work, the influence of hydrodynamic lubrication force models on the dynamic of the slider crank mechanism was investigated. From the numerical simulations performed it can be noticed that all lubrication models introduce changes on the dynamic response of the mechanism. Particularly for short bearings the analytical solution predicts higher peaks in acceleration and force values.

For long bearings, the overall performance of the mechanism was similar for both analytical and numerical solutions, with minor differences on the thickness of fluid film. Finally, these results show the importance of the choice of the lubrication force model to the development of a more complete analytical model as well as an elastohydrodynamic lubrication scheme to predict more accurately the complex lubrication regime present in these machines, especially for short bearings. Moreover, the correct prediction of the hydrodynamic conditions in the lubricated revolute joint is very important due to its strong influence in the fault evaluation, such as cavitation of the oil, film, deformation and bearing wear.

5. ACKNOWLEDGEMENTS

The authors would like to thank the CAPES for the financial support of this research.

6. REFERENCES

Bannwart, A.C., Cavalca, K.L. and Daniel, G.B., 2010. "Hydrodynamic bearings modeling with alternate motion". *Mechanics Research Communications*, Vol. 37, No. 6, pp. 590–597.

Daniel, G.B.; Cavalca, K.L. Analysis of the dynamics of a slider-crank mechanism with hydrodynamic lubrication in the connecting rod-slider joint clearance. Mechanism and Machine Theory, v. 46, 2011, p. 1434–1452.

Dowson, D., "A Generalized Reynolds Equation for Fluid Film Lubrication", International Journal of Mechanical Sciences, Volume 4, Issues 2, 1962, pp. 159-170.

Flores, P., Ambrósio, J. and Claro, J.P., 2004. "Dynamic analysis for planar multibody mechanical systems with lubricated joints". *Multibody System Dynamics*, Vol. 12, No. 1, pp. 47–74.

Flores, P., Ambrósio, J., Claro, J.C.P., Lankarani, H. and Koshy, C., 2009. "Lubricated revolute joints in rigid multibody systems". *Nonlinear Dynamics*, Vol. 56, No. 3, pp. 277–295.

Flores, P., Koshy, C., Lankarani, H., Ambrósio, J. and Claro, J.C.P., 2011. "Numerical and experimental investigation on multibody systems with revolute clearance joints". *Nonlinear Dynamics*, Vol. 65, No. 4, pp. 383–398.

Frêne, J., Nicolas, D., Degneurce, B., Berthe, D., Godet, M.: Hydrodynamic Lubrication. Bearings and Thrust Bearings. Elsevier, Amsterdam (1997).

Pinkus, O., Sternlicht, S.A.: Theory of Hydrodynamic Lubrication. McGraw Hill, New York (1961).

Machado, M., Costa, J., Seabra, E. and Flores, P., 2012. "The effect of the lubricated revolute joint parameters and hydrodynamic force models on the dynamic response of planar multibody systems". *Nonlinear Dynamics*, Vol. 69, No. 1-2, pp. 635–654.

Maliska, C. R., 2004, "Transferência de Calor e Mecânica dos Fluidos Computacional", 2ª Ed, Livros Técnicos e Científicos Editora SA, Rio de Janeiro, RJ, Brasil.

Reis, V. L., Daniel, G. B., Cavalca, K. L. Dynamic analysis of a lubricated planar slider–crank mechanism considering friction and Hertz contact effects, Mechanism and Machine Theory, Vol. 74, 2014, p. 257–273.

Reynolds, O., On the Theory of Lubrication and its Application to Mr. Beauchamp Tower's Experiments, including an Experimental Determination of the Viscosity of Olive Oil. Philosophical Transactions of Royal Society of London, Series A, 1886, Vol. 177, Part 1, pp.157-234.

Shampine, L.F.; Gordon, M.K. Computer solution of ordinary differential equations: The initial value problem, W.H.Freeman & Co Ltd., 1975

Tian, Q., Liu, C., Machado, M. and Flores, P., 2011. "A new model for dry and lubricated cylindrical joints with clearance in spatial flexible multibody systems". Nonlinear Dynamics, Vol. 64, No. 1-2, pp. 25–47.

Tian, Q., Sun, Y., Liu, C., Hu, H. and Flores, P., 2013. "Elastohydrodynamic lubricated cylindrical joints for rigid-flexible multibody dynamics". *Computers & Structures*, Vol. 114-115, No. 0, pp. 106 – 120.

7. RESPONSIBILITY NOTICE

The authors are the only responsible for the printed material included in this paper.